Journal of Solid State Chemistry 184 (2011) 1671–1681

Contents lists available at ScienceDirect

Journal of Solid State Chemistry

journal homepage: www.elsevier.com/locate/jssc

New members of ternary rare-earth metal boride carbides containing finite boron–carbon chains: $RE_{25}B_{14}C_{26}$ (RE=Pr, Nd) and $Nd_{25}B_{12}C_{28}$

Volodymyr Babizhetskyy [a,b,*], Hansjürgen Mattausch [a], Arndt Simon [a], Régis Gautier [c,**], Jean-François Halet [c,***]

[a] Max-Planck-Institut für Festkörperforschung, Heisenbergstrasse 1, Postfach 800665, D-70569 Stuttgart, Germany
[b] Department of Inorganic Chemistry, Ivan Franko National University of Lviv, Kyryla & Mefodiya Street 6, UA-79005 Lviv, Ukraine
[c] Sciences Chimiques de Rennes, UMR 6226 CNRS, Ecole Nationale Supérieure de Chimie de Rennes, Université de Rennes 1, Avenue du Général Leclerc, F-35042 Rennes cedex, France

ARTICLE INFO

Article history:
Received 17 March 2011
Received in revised form
17 April 2011
Accepted 24 April 2011
Available online 30 April 2011

Dedicated to Prof. Hansgeorg Schnöckel on the Occasion of his 70th Birthday

Keywords:
Rare-earth metal boride carbide
Crystal structure
Electronic structure
Extended Hückel tight-binding calculations

ABSTRACT

New ternary rare-earth metal boride carbides $RE_{25}B_{14}C_{26}$ (RE=Pr, Nd) and $Nd_{25}B_{12}C_{28}$ were synthesized by co-melting the elements. $Nd_{25}B_{12}C_{28}$ is stable up to 1440 K. $RE_{25}B_{14}C_{26}$ (RE=Pr, Nd) exist above 1270 K. The crystal structures were investigated by means of single-crystal X-ray diffraction. $Nd_{25}B_{12}C_{28}$: space group $P\bar{1}$, a=8.3209(7) Å, b=8.3231(6) Å, c=29.888(2) Å, α=83.730(9)°, β=83.294(9)°, γ=89.764(9)°. $Pr_{25}B_{14}C_{26}$: space group $P2_1/c$, a=8.4243(5) Å, b=8.4095(6) Å, c=30.828(1) Å, β=105.879(4)°, V=2100.6(2) Å^3, ($R1$=0.048 (w$R2$=0.088) from 2961 reflections with $I_o > 2\sigma(I_o)$); for $Nd_{25}B_{14}C_{26}$ space group $P2_1/c$, Z=2, a=8.3404(6) Å, b=8.3096(6) Å, c=30.599(2) Å, β=106.065(1)°. Their structures consist of a three-dimensional framework of rare-earth metal atoms resulting from the stacking of slightly corrugated and distorted square nets, leading to cavities filled with cumulene-like molecules $[B_2C_4]^{6-}$ and $[B_3C_3]^{7-}$, nearly linear $[BC_2]^{5-}$ and bent $[BC_2]^{7-}$ units and isolated carbon atoms. Structural and theoretical analysis suggests the ionic formulation for $RE_{25}B_{14}C_{26}$: $(RE^{3+})_{25}[B_2C_4]^{6-}([B_3C_3]^{7-})_2([BC_2]^{5-})_4([BC_2]^{7-})_2(C^{4-})_4 \cdot 5e^-$ and for $Nd_{25}B_{12}C_{28}$: $(Nd^{3+})_{25}([B_2C_4]^{6-})_3([BC_2]^{5-})_4([BC_2]^{7-})_2(C^{4-})_4 \cdot 7e^-$. Accordingly, extended Hückel tight-binding calculations indicate that the compounds are metallic in character.

1. Introduction

The structures of ternary the rare-earth (RE) metal boride carbides $RE_xB_yC_z$ display a variety of different arrangements with boron–carbon substructures ranging from zero-dimensional units to one-dimensional chains and two-dimensional networks embedded in the metal atom sublattice as well as interconnected boron icosahedra in the case of high boron content [1,2]. Compounds can be separated into different categories, depending upon the structural arrangement of the non-metal atoms. The first category contains finite quasi-molecular entities of different lengths ranging from 2 to 13 non-metal atoms. Different sizes as well as isolated C atoms can coexist in some compounds [1,3–5]. In the second category, the non-metal atoms form infinite one-dimensional planar or nearly planar ribbons $(BC)_\infty$ zigzag chains of boron atoms to which carbon atoms are attached [1,6]. In structures of the third category, the boron and carbon atoms form infinite, planar layers [1,7]. The dimensionality of the boron–carbon network is related to the average valence electron concentration (VEC) per main group atom [7], assuming a Zintl–Klemm ionic bonding scheme [8] between the metal and the non-metal atoms as a first approximation.

Compounds belonging to the first category have generally a VEC larger than 5. About ten types of structures have already been structurally characterized in this family. Besides single carbon atoms, nine types of finite quasi-molecular boron–carbon units with different boron/carbon ratio have been found so far (see Table 1). Inside the family itself, the number of bonding contacts between boron and carbon atoms generally diminishes when the VEC increases. Short three-atom BC_2 entities are found in compounds such as Sc_2BC_2 (VEC=5.67) [9], $RE_5B_2C_5$ (VEC=5.86) [10], $RE_{15}B_4C_{14}$ (VEC=6.28) [11] and Lu_3BC_3 (VEC=6.00) [12] as well as $Sc_3B_{0.75}C_3$ [13]. Four-atom B_2C_2 groups are found in the compounds RE_2BC (VEC=6.50) [14]. $RE_5B_2C_6$ (VEC=5.63) [15,10] contains BC_3 units and isolated carbon atoms. Longer oligomeric anions are observed when the boron–carbon ratio increases such as in $La_{15}B_{14}C_{19}$ (VEC=4.94) [16], which contains 11-membered B_4C_7 and B_5C_6 units, as well as in $RE_{10}B_9C_{12}$ (VEC=5.00) [17], where 13-membered B_5C_8 units, the longest so far observed in these compounds, and 8-membered B_4C_4 units occur. $RE_5B_4C_5$

* Corresponding author at: Ivan Franko National University of Lviv, Department of Inorganic Chemistry, Kyryla & Mefodiya Str. 6, 79005 Lviv, Ukraine. Fax: +49 711 689 16 42.
** Corresponding author.
*** Corresponding author. Fax: +33 2 2323 6840.
E-mail addresses: v.babizhetskyy@googlemail.com (V. Babizhetskyy), rgautier@ensc-rennes.fr (R. Gautier), halet@univ-rennes1.fr (J.-F. Halet).

0022-4596/$ - see front matter © 2011 Elsevier Inc. All rights reserved.
doi:10.1016/j.jssc.2011.04.039

Table 1
Different finite B, C units in rare-earth metal boron carbides *RExByCz*, structurally characterized.

Structural type	VEC[a]	B–C network	Ref.
La15B14C19	4.94	[B4C7][B5C6]	[16]
LaBC (Ce, Pr, Nd, Sm)	5.00	$[B_5C_5]$	[19]
Ce10B9C12 (La, Pr, Nd)	5.00	[B5C8][B4C4]	[17]
Ce5B4C5 (La, Pr, Nd)	5.22	[B4C4][B3C3][BC2][C]	[18]
La5B2C6 (Ce, Nd, Gd, Ho)	5.63	[BC3][C]	[12,10]
Sc2BC2 (Nd)	5.67	[BC2]	[9]
Gd5B2C5 (Sm)	5.86	[BC2][C]	[10]
$Pr_{15}B_6C_{20}$ (Nd)	5.50	$[B_2C_4][C_3][C]$	[20]
$Nd_{25}B_{14}C_{26}$	5.53	$[B_2C_4][B_3C_3][BC_2][C]$	This work
$Nd_{25}B_{12}C_{28}$	5.57	$[B_2C_4][BC_2][C]$	This work
Lu_3BC_3	6.00	$[BC_2][C]$	[12]
$Sc_3B_{0.75}C_3$	6.20	$[BC_2][C]$	[13]
$Tb_{15}B_4C_{14}$ (Er)	6.28	$[BC_2][C]$	[11]
Nd_2BC (Pr)	6.50	$[B_2C_2]$	[14,21]

[a] Averaged valence electron count per main group atom calculated assuming trivalent metals.

(VEC=5.22) [18] contains 3-membered BC_2, 6-membered B_3C_3, and 8-membered B_4C_4 units, in addition to single C atoms, and in the LaBC-type of structure (VEC=5.00) only B_5C_5 units were found [19]. Recently we have also reported new 6-membered B_2C_4 entities in $RE_{15}B_6C_{20}$ (*RE*=Pr, Nd) (VEC=5.50) [20].

Two new closely related structural representatives of this category were discovered during our investigations of the Pr–B–C and Nd–B–C systems [21]. Here we report the synthesis, crystal structure and electronic structure of these compounds, namely $Nd_{25}B_{12}C_{28}$ (VEC=5.57) and $RE_{25}B_{14}C_{26}$ (*RE*=Pr, Nd) (VEC=5.53).

2. Experimental

2.1. Synthesis and analysis

The samples of $RE_{25}B_{14}C_{26}$ (*RE*=Pr, Nd) and $Nd_{25}B_{12}C_{28}$ were prepared from commercially available pure elements: rare-earth metals with a claimed purity of 99.99 at%, Alfa—Aesar, Johnson Matthey Company, sublimed bulk pieces; crystalline boron powder, purity 99.99 at%, H.C. Starck, Germany; graphite powder, purity 99.98 at%, Aldrich. The pellets were arc-melted under purified argon atmosphere on a water-cooled copper hearth. The alloy buttons of ~1 g were turned over and remelted three times to improve homogeneity. Subsequent heating just above the melting point was carried out in a high-frequency furnace (TIG-10/300, Hüttinger, FRG) under argon atmosphere for 24 h at 1350, 1670 and 1550 K for $Pr_{25}B_{14}C_{26}$, $Nd_{25}B_{14}C_{26}$ and $Nd_{25}B_{12}C_{28}$ containing samples, respectively. Finally, the samples were wrapped in molybdenum foils, annealed in evacuated silica tubes for one month at 1270 K and subsequently quenched in cold water. Sample handling was carried out under argon atmosphere in a glove box or through the Schlenk technique.

Before annealing metallographic and X-ray diffraction analyses of the samples with different atomic ratios show the new compound $Pr_{25}B_{14}C_{26}$ to be present with varying amounts of $Pr_5B_4C_5$ [18] and Pr. After annealing at 1270 K the phase $Pr_{25}B_{14}C_{26}$ has vanished and only $Pr_5B_2C_5$ [22] and Pr_2BC [21] are detected. The new compound $Nd_{25}B_{14}C_{26}$ coexist with varying amounts of $Nd_{10}B_9C_{12}$ [17] and NdBC [19] before annealing. After annealing at 1270 K $Nd_{25}B_{14}C_{26}$ has transformed into NdBC [19] and $Nd_5B_4C_5$ [18]. Hence, both phases $RE_{25}B_{14}C_{26}$ (*RE*=Pr, Nd) exist above 1270 K. The nearly placed new compound $Nd_{25}B_{12}C_{28}$ coexist with varying amounts of $Nd_5B_4C_5$ [18] and $Nd_5B_2C_6$ [10] before annealing. After annealing at 1270 K $Nd_{25}B_{12}C_{28}$ has transformed into $Nd_5B_2C_6$ [10] and $Nd_5B_2C_5$ [10], also beside elemental Nd. The phases formed after annealing correspond to the phase equilibria observed at 1270 K [21].

2.2. X-ray diffraction and structure refinement

X-ray powder diffraction patterns were obtained on a diffractometer STOE STADI P with Mo$K\alpha_1$ radiation, using capillaries sealed under argon to avoid hydrolysis. The correct indexing and refining of the diffraction patterns was ensured with the help of the WinCSD program package [23] and by intensity calculations taking the atomic positions from the refined structures of $RE_{25}B_{14}C_{26}$ (*RE*=Pr, Nd) and $Nd_{25}B_{12}C_{28}$. The unit cell parameters refined from X-ray powder data are: $a=8.430(2)$ Å, $b=8.419(2)$ Å, $c=30.860(3)$ Å, $\beta=105.92(1)^\circ$, $V=2106(1)$ Å^3, for $Pr_{25}B_{14}C_{26}$; $a=8.345(2)$ Å, $b=8.311(1)$ Å, $c=30.632(3)$ Å, $\beta=106.08(1)^\circ$, $V=2041(1)$ Å^3 for $Nd_{25}B_{14}C_{26}$ and $a=8.321(1)$ Å, $b=8.316(1)$ Å, $c=29.981(3)$ Å, $\alpha=83.56(2)^\circ$, $\beta=83.00(2)^\circ$, $\gamma=89.79(1)^\circ$, $V=2046(1)$ Å^3 for $Nd_{25}B_{12}C_{28}$. The calculated X-ray powder pattern for the obtained crystal structure is in the good agreement with the experimental pattern (Fig. 1).

Small and irregularly shaped single crystals were selected for X-ray investigation from crushed but not annealed samples. The crystals were first examined by Buerger's precession technique in order to establish their suitability for intensity collection. Single-crystal intensity data of $RE_{25}B_{14}C_{26}$ (*RE*=Pr, Nd) and $Nd_{25}B_{12}C_{28}$ were collected at room temperature on STOE IPDS I and STOE IPDS II image plate diffractometer with monochromatized Ag$K\alpha$ and Mo$K\alpha$ radiation by oscillation of the crystal around the ω axis. The starting atomic parameters derived via direct methods using the program SIR 97 [24] were subsequently refined with the program SHELX-97 [25] (full-matrix least-squares on F^2) with anisotropic atomic displacements for all atoms for $Nd_{25}B_{14}C_{26}$ and for *RE* atoms for $Pr_{25}B_{14}C_{26}$ and $Nd_{25}B_{12}C_{28}$ within the WinGX program package [26]. All relevant crystallographic results for the data collections and evaluations are listed in Tables 2–5.

The refinements converge well, but they indicate inconsistencies. Some atomic metal atom positions in the crystal structures are not fully occupied. In the structure of $Nd_{25}B_{12}C_{28}$ the anisotropic displacement parameters of Nd10, Nd16 and Nd21 show large values along the *c* direction. We therefore refined these atoms with split positions, Nd10/Nd27, Nd21/Nd28 and Nd16/Nd29 with the occupation factors listed in Table 3. A similar

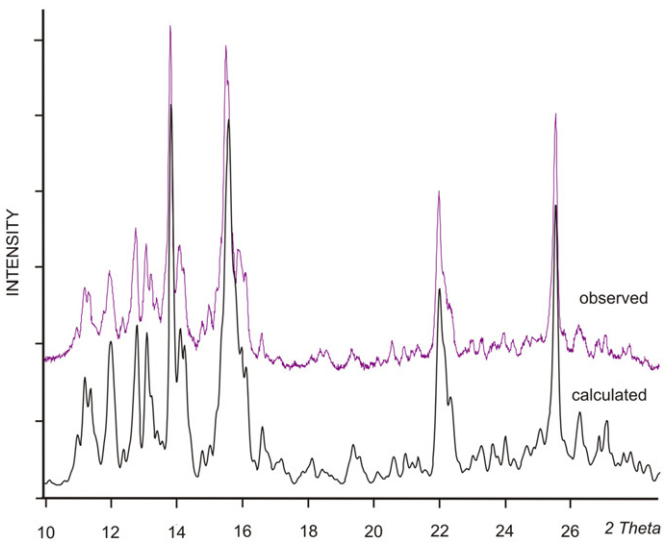

Fig. 1. Observed and calculated powder patterns of $Nd_{25}B_{12}C_{28}$ (Mo$K\alpha_1$ radiation).

Table 2
Crystal data and structure refinement for $RE_{25}B_{14}C_{26}$ (RE=Pr, Nd) and $Nd_{25}B_{12}C_{28}$.

Empirical formula	$Pr_{25}B_{14}C_{26}$	$Nd_{25}B_{14}C_{26}$	$Nd_{25}B_{12}C_{28}$
Crystal system:	Monoclinic	Monoclinic	Triclinic
Space group:	$P2_1/c$ (No. 14)	$P2_1/c$ (No. 14)	P-1 (No. 2)
Pearson's symbol	mP134	mP134	aP136
Formula per unit cell (Z)	2	2	2
Lattice parameters			
a (Å)	8.4243(5)	8.3404(6)	8.3209(7)
b (Å)	8.4095(6)	8.3096(6)	8.3231(6)
c (Å)	30.828(1)	30.599(2)	29.888(2)
α (deg)			83.730(9)
β (deg)	105.879(4)	106.065(1)	83.294(9)
γ (deg)			89.764(9)
Unit cell volume (Å)^3	2100.6(2)	2037.9(2)	2043.4(3)
Calculated density (g/cm^3)	6.302	6.632	6.618
Absorption coefficient (1/cm)	28.362	16.353	16.519
Crystal size (mm^3)	$0.095 \times 0.062 \times 0.044$	$0.085 \times 0.048 \times 0.018$	$0.075 \times 0.050 \times 0.037$
Radiation and wavelength (Å)	Mo $K\alpha$, 0.71069	Ag $K\alpha$, 0.56083	Ag $K\alpha$, 0.56083
Diffractometer	STOE IPDS II	STOE IPDS I	STOE IPDS I
Refined parameters	200	299	401
Refinement	F^2	F^2	F^2
$2\theta_{max}$ and $(\sin\theta/\lambda)_{max}$	52.74, 0.566	56.4, 0.754	44.54, 0.611
h, k, l	$-10<h<10$	$-13<h<13$	$-11<h<11$
	$-10<k<10$	$-13<k<13$	$-11<k<11$
	$-38<l<35$	$-51<l<51$	$-40<l<40$
Collected reflections	14,021	45,066	25,295
Independent reflections	3830 (R_{int}=0.051)	10,091 (R_{int}=0.065)	9548 (R_{int}=0.052)
Reflections with $I_o > 2\sigma(I_o)$	2961 (R_σ=0.037)	7482(R_σ=0.039)	7339(R_σ=0.045)
Final (R_1[a]) indices (R_1[a]) all data	0.048 (0.069)	0.035 (0.055)	0.048 (0.066)
Weighted (wR_2[b]) factor(wR_2[b]) all data	[c]0.088 (0.094)	[d]0.077 (0.085)	[e]0.123 (0.134)
Goodness-of-fit on F^2:	1.21	1.03	1.09
Extinction coefficient	0.00013(2)	None	None
Largest diff.peak and hole (e/Å^{-3})	2.07/−1.60	4.2/−3.7	2.76/−3.16

[a] $R_1(F)=[\Sigma(|F_o|-|F_c|)]/\Sigma|F_o|$.
[b] $wR_2(F^2)=[\Sigma[w(F_o^2-F_c^2)^2/\Sigma[w(F_o^2)^2]]]^{1/2}$.
[c] $[w^{-1}=\sigma^2(F_o)^2+(0.023\ P)^2+93.82\ P]$, where $P=(F_o^2+2F_c^2)/3$.
[d] $[w^{-1}=\sigma^2(F_o)^2+(0.038P)^2+16.03P]$, where $P=(F_o^2+2F_c^2)/3$.
[e] $[w^{-1}=\sigma^2(F_o)^2+(0.075\ P)^2+14.69\ P]$, where $P=(F_o^2+2F_c^2)/3$.

Table 3
Atomic coordinates and isotropic displacement parameters (in Å^2) for $Nd_{25}B_{12}C_{28}$.

Atom	Site	Occ	x	y	z	U_{eq}
Nd1	2(i)	1	−0.24237(7)	−0.04386(7)	0.61105(2)	0.0049(1)
Nd2	2(i)	1	−0.08340(7)	0.12530(7)	0.19711(2)	0.0060(1)
Nd3	2(i)	1	−0.15120(7)	−0.15091(7)	0.38789(2)	0.0047(1)
Nd4	2(i)	1	−0.44511(7)	0.34368(7)	0.61175(2)	0.0050(1)
Nd5	2(i)	1	−0.47224(7)	0.31849(7)	0.19577(2)	0.0057(1)
Nd6	2(i)	1	−0.66817(7)	−0.07418(7)	0.19756(2)	0.0083(1)
Nd7	2(i)	1	−0.27577(7)	−0.26760(7)	0.19539(2)	0.0059(1)
Nd8	2(i)	1	0.11313(7)	0.71191(7)	0.48162(2)	0.0086(1)
Nd9	2(i)	1	−0.40401(7)	0.80776(7)	−0.00080(2)	0.0074(1)
Nd10	2(i)	0.546(9)	0.1214(6)	0.5232(6)	0.2013(2)	0.0062(6)
Nd11	2(i)	1	0.04478(7)	0.45047(7)	0.39541(2)	0.0072(1)
Nd12	2(i)	1	−0.54519(7)	0.65338(7)	0.11187(2)	0.0062(1)
Nd13	1(a)	1	0	0	0	0.0099(2)
Nd14	2(i)	1	0.17827(7)	−0.22509(7)	0.30812(2)	0.0063(1)
Nd15	2(i)	1	−0.74519(7)	0.26393(7)	0.11297(2)	0.0063(1)
Nd16	2(i)	0.80(2)	−0.3596(1)	−0.7506(1)	0.3916(2)	0.0051(5)
Nd17	2(i)	1	0.06500(7)	−0.14315(7)	0.11250(2)	0.0062(1)
Nd18	2(i)	1	−0.30944(7)	−0.09501(7)	0.49931(2)	0.0075(1)
Nd19	2(i)	1	−0.21593(7)	−0.41750(7)	0.30303(2)	0.0055(1)
Nd20	2(i)	1	−0.41564(7)	−0.01157(7)	0.29563(2)	0.0059(1)
Nd21	2(i)	0.45(2)	−0.195(1)	0.403(2)	−0.0192(3)	0.0072(8)
Nd22	2(i)	1	−0.02249(7)	−0.80891(7)	0.30504(2)	0.0051(1)
Nd23	2(i)	1	−0.13670(7)	0.46259(7)	0.10871(2)	0.0077(1)
Nd24	2(i)	1	−0.33403(8)	0.06109(8)	0.10276(3)	0.0148(2)
Nd25	2(i)	1	0.37609(7)	−0.61883(7)	0.30471(2)	0.0055(1)
Nd26	1(h)	1	−1/2	1/2	1/2	0.0139(2)
Nd27	2(i)	0.454(9)	0.1198(7)	0.5212(8)	0.2141(2)	0.0062(6)
Nd28	2(i)	0.55(2)	−0.199(1)	0.394(1)	−0.0092(3)	0.0072(8)

Table 3 (*continued*)

Atom	Site	Occ	*x*	*y*	*z*	U_{eq}
Nd29	2(*i*)	0.20(2)	−0.3610(8)	−0.7505(8)	0.4043(5)	0.0051(5)
C1	2(*i*)	1	0.143(1)	−0.251(1)	0.3877(4)	0.007(2)
C2	2(*i*)	1	−0.043(1)	0.158(1)	0.1181(4)	0.007(2)
C3	2(*i*)	1	0.021(1)	0.823(1)	0.2048(4)	0.009(2)
C4	2(*i*)	1	−0.577(1)	−0.382(1)	0.2028(4)	0.011(2)
C5	2(*i*)	1	−0.238(1)	−0.245(1)	0.1152(4)	0.008(2)
C6	2(*i*)	1	0.221(1)	0.221(1)	0.2055(4)	0.012(2)
C7	2(*i*)	1	−0.441(1)	0.353(1)	0.1158(4)	0.0059(9)
C8	2(*i*)	1	0.344(1)	−0.643(1)	0.3846(4)	0.008(2)
C9	2(*i*)	1	0.278(1)	−0.914(1)	0.2957(4)	0.010(2)
C10	2(*i*)	1	0.479(1)	−0.311(1)	0.2938(4)	0.007(2)
C11	2(*i*)	1	−0.113(1)	−0.111(1)	0.2958(4)	0.010(2)
C12	2(*i*)	1	−0.249(1)	−0.446(1)	0.3823(4)	0.008(2)
C13	2(*i*)	1	−0.055(1)	−0.844(1)	0.3847(4)	0.007(2)
C14	2(*i*)	1	−0.179(2)	0.429(2)	0.2028(5)	0.016(2)
C15	2(*i*)	1	−0.450(1)	−0.041(1)	0.3781(4)	0.009(2)
C16	2(*i*)	1	0.084(2)	−0.514(2)	0.3017(5)	0.021(3)
C17	2(*i*)	1	−0.638(1)	−0.042(1)	0.1173(4)	0.012(2)
C18	2(*i*)	1	−0.375(2)	0.023(2)	0.1968(5)	0.021(3)
C19	2(*i*)	1	−0.840(2)	0.554(2)	0.1177(6)	0.028(3)
C20	2(*i*)	1	−0.320(2)	−0.712(2)	0.2934(5)	0.018(3)
C21	2(*i*)	1	−0.500(1)	0.517(1)	−0.0248(4)	0.008(2)
C22	2(*i*)	1	−0.783(1)	0.401(1)	0.4766(4)	0.009(2)
C23	2(*i*)	1	−0.118(1)	0.696(1)	0.0241(4)	0.011(2)
C24	2(*i*)	1	−0.808(1)	0.406(1)	0.5273(4)	0.012(2)
C25	2(*i*)	1	−0.077(1)	0.715(1)	−0.0266(4)	0.012(2)
C26	2(*i*)	1	−0.004(1)	−0.024(1)	0.5249(4)	0.011(2)
C27	2(*i*)	1	−0.590(2)	−0.174(2)	0.4650(5)	0.019(3)
C28	2(*i*)	1	−0.294(2)	0.117(2)	−0.0331(6)	0.024(3)
B1	2(*i*)	1	0.061(1)	−0.108(1)	0.5666(4)	0.008(2)
B2	2(*i*)	1	0.318(2)	−0.640(2)	0.4334(5)	0.011(2)
B3	2(*i*)	1	−0.258(1)	−0.451(2)	0.4304(5)	0.009(2)
B4	2(*i*)	1	−0.008(2)	0.191(2)	0.0682(5)	0.012(2)
B5	2(*i*)	1	−0.046(1)	−0.150(2)	0.2508(4)	0.008(2)
B6	2(*i*)	1	−0.491(2)	−0.075(2)	0.4274(5)	0.014(3)
B7	2(*i*)	1	−0.194(2)	−0.235(2)	0.0657(5)	0.015(3)
B8	2(*i*)	1	−0.445(2)	0.387(2)	0.0659(5)	0.011(2)
B9	2(*i*)	1	−0.555(2)	−0.343(2)	0.2492(4)	0.008(2)
B10	2(*i*)	1	0.254(2)	0.159(1)	0.2501(5)	0.009(2)
B11	2(*i*)	1	−0.637(2)	−0.051(2)	0.0693(6)	0.022(3)
B12	2(*i*)	1	−0.240(2)	0.355(2)	0.2492(5)	0.015(3)

situation was observed in the structures of both $RE_{25}B_{14}C_{26}$ (*RE*=Pr, Nd) concerning the positions Pr12 and Nd12 which had to be split into *RE*12/*RE*13, see Tables 4 and 5. The light atoms were located from the difference Fourier maps, and the final difference Fourier analyses gave no indications for additional atomic sites for both types of structures. At the beginning of the structure solution for $RE_{25}B_{14}C_{26}$ (*RE*=Pr, Nd) the asymmetrical 6-atom unit was refined as B_2C_4. The large displacement parameters of the carbon atom position and the distance to the neighbor B2 atom of 1.57 Å lead to the composition B_3C_3. The atomic coordinates and thermal parameters of $RE_{25}B_{14}C_{26}$ (*RE*=Pr, Nd) and $Nd_{25}B_{12}C_{28}$ are listed in Tables 3–5, respectively. Selected interatomic distances of $Nd_{25}B_{14}C_{26}$ and $Nd_{25}B_{12}C_{28}$ are reported in Tables 6 and 7. The program DIAMOND was used for drawing of crystal structures [27]. Crystal structures of $RE_{25}B_{14}C_{26}$ and $Nd_{25}B_{12}C_{28}$ along [0 1 0] are presented in Fig. 2. Rare-earth metal atom environments of the finite boron–carbon entities in $Nd_{25}B_{14}C_{26}$ are shown in Fig. 3. Analogous metal surrounding is encountered for $Nd_{25}B_{12}C_{28}$.

2.3. Theoretical calculations

All molecular and tight-binding calculations have been carried out within the extended Hückel (EH) formalism [28] with the YAeHMOP software [29]. Nd-containing crystal structures were considered. Because of the fractional occupation of some Nd crystallographic positions, several structural models using these different positions were taken into account. For each compound, theoretical results remained unchanged regardless of the structural model considered. EH atomic parameters of lanthanum were used. The role of contracted *f* orbitals for La was neglected, and thus they were not included in the calculations. The exponents (ζ) and the valence shell ionization potentials (H_{ii} in eV) were (respectively): 1.3 and −15.2 for B 2*s*, 1.3 and −8.5 for B 2*p*, 1.625 and −21.4 for C 2*s*, 1.625 and −11.4 for C 2*p*, 2.14 and −7.67 for La 6*s*, 2.08 and −5.01 for La 6*p*. H_{ii} values for La 5*d* were set equal to −8.21. A linear combination of two Slater-type orbitals of exponents ζ_1= 3.780 and ζ_2=1.811 with the weighting coefficients c_1=0.7765 and c_2=0.4586, respectively, was used to represent the La 5*d* atomic orbitals. The density of states (DOS) and crystal orbital overlap populations (COOP) were obtained using a set of 8*k* points of the irreducible wedge of the Brillouin zone.

3. Results and discussion

3.1. Structural characterization

The rare-earth metal sub-lattice of $RE_{25}B_{14}C_{26}$, (*RE*=Pr, Nd) and $Nd_{25}B_{12}C_{28}$ consists of a three-dimensional framework resulting from the stacking of slightly corrugated and distorted square nets along the [0 0 1] direction and rotated to each other by about

Table 4
Atomic coordinates and isotropic displacement parameters (in Å^2) for $Pr_{25}B_{14}C_{26}$.

Atom	Site	Occ	x	y	z	U_{eq}
Pr1	4*e*	1	−0.0064(1)	0.0070(1)	0.19728(3)	0.0085(2)
Pr2	4*e*	1	0.2028(1)	0.1161(1)	0.30465(3)	0.0077(2)
Pr3	4*e*	1	0.6008(1)	0.3048(1)	0.30348(3)	0.0079(2)
Pr4	4*e*	1	−0.1919(1)	0.3067(1)	0.11201(3)	0.0073(2)
Pr5	4*e*	1	0.2041(1)	0.4099(1)	0.20470(3)	0.0079(2)
Pr6	4*e*	1	−0.3978(1)	−0.0898(1)	0.10486(3)	0.0090(2)
Pr7	4*e*	1	0.2120(1)	0.1129(1)	0.11211(3)	0.0071(2)
Pr8	4*e*	1	−0.1893(1)	0.4037(1)	0.00071(3)	0.0087(2)
Pr9	4*e*	1	0.4135(1)	0.5012(1)	0.11126(3)	0.0066(2)
Pr10	4*e*	1	−0.5888(1)	0.2049(1)	0.01785(4)	0.0111(2)
Pr11	4*e*	1	0.5922(1)	0.2007(1)	0.19254(3)	0.0092(2)
Pr12	4*e*	0.82(3)	−0.0121(6)	0.2083(3)	0.3916(4)	0.0073(9)
Pr13	4*e*	0.18(3)	0.006(2)	0.213(1)	0.4045(8)	0.0073(9)
Pr14	2*a*	1	0	0	0	0.0132(3)
C1	4*e*	1	−0.281(2)	0.615(2)	0.1154(5)	0.007(3)
C2	4*e*	1	0.137(3)	0.316(3)	0.0349(8)	0.019(4)
C3	4*e*	1	0.318(2)	−0.186(2)	0.1164(6)	0.012(3)
C4	4*e*	1	0.106(2)	0.706(2)	0.2066(7)	0.019(4)
C5	4*e*	1	−0.097(2)	0.310(2)	0.2033(6)	0.015(3)
C6	4*e*	1	0.505(2)	0.506(2)	0.2033(5)	0.006(3)
C7	4*e*	1	0.119(2)	0.412(2)	0.1226(6)	0.009(3)
C8	4*e*	1	0.308(2)	0.409(2)	0.3049(6)	0.017(4)
C9	4*e*	1	−0.320(2)	0.106(2)	−0.0240(6)	0.009(3)
C10	4*e*	1	0.512(2)	0.207(2)	0.1124(5)	0.005(3)
C11	4*e*	1	−0.086(2)	0.008(2)	0.1176(6)	0.007(3)
C12	4*e*	1	0.692(2)	0.609(2)	0.2934(6)	0.012(3)
C13	4*e*	1	−0.466(2)	0.515(2)	0.0241(6)	0.012(3)
B1	4*e*	1	0.598(2)	0.559(2)	0.2487(7)	0.010(4)
B2	4*e*	1	−0.146(2)	0.020(2)	0.0701(7)	0.012(4)
B3	4*e*	1	0.098(2)	0.758(2)	0.2519(7)	0.012(4)
B4	4*e*	1	−0.347(2)	0.581(2)	0.0666(6)	0.008(3)
B5	4*e*	1	0.278(3)	−0.169(3)	0.0678(8)	0.020(4)
B6	4*e*	1	0.096(2)	0.392(2)	0.0739(8)	0.013(4)
B7	4*e*	1	−0.271(2)	0.077(2)	0.0255(7)	0.012(4)

Table 5
Atomic coordinates and isotropic displacement parameters (in Å^2) for. $Nd_{25}B_{14}C_{26}$.

Atom	Site	Occ	x	y	z	U_{eq}
Nd1	4*e*	1	−0.00799(4)	0.00590(4)	0.197143(9)	0.00928(5)
Nd2	4*e*	1	0.20358(4)	0.11639(4)	0.304667(9)	0.00864(5)
Nd3	4*e*	1	0.59991(4)	0.30508(4)	0.303628(9)	0.00932(5)
Nd4	4*e*	1	−0.19164(4)	0.30590(4)	0.112180(9)	0.00806(5)
Nd5	4*e*	1	0.20424(4)	0.40939(4)	0.20497(1)	0.00954(5)
Nd6	4*e*	1	−0.39724(4)	−0.08954(4)	0.10522(1)	0.01025(5)
Nd7	4*e*	1	0.21293(4)	0.11258(4)	0.112051(9)	0.00809(5)
Nd8	4*e*	1	−0.18983(4)	0.40433(4)	0.00066(1)	0.01042(6)
Nd9	4*e*	1	0.41388(4)	0.50035(4)	0.111309(9)	0.00793(5)
Nd10	4*e*	1	−0.58676(4)	0.20484(4)	0.01887(1)	0.01068(6)
Nd11	4*e*	1	0.59208(4)	0.19943(4)	0.19209(1)	0.00925(5)
Nd12	4*e*	0.774(5)	−0.01366(9)	0.20750(7)	0.39084(5)	0.0077(1)
Nd13	4*e*	0.226(5)	0.0031(3)	0.2103(3)	0.4029(1)	0.0077(1)
Nd14	2*a*	1	0	0	0	0.01547(9)
C1	4*e*	1	−0.2825(7)	0.6109(7)	0.1147(2)	0.0099(9)
C2	4*e*	1	0.135(1)	0.312(1)	0.0334(3)	0.019(1)
C3	4*e*	1	0.3196(7)	−0.1897(7)	0.1161(2)	0.0102(8)
C4	4*e*	1	0.1061(8)	0.7079(8)	0.2053(2)	0.015(1)
C5	4*e*	1	−0.1001(8)	0.3080(8)	0.2036(2)	0.014(1)
C6	4*e*	1	0.5070(7)	0.5039(7)	0.2029(2)	0.0098(9)
C7	4*e*	1	0.1212(8)	0.4104(8)	0.1216(2)	0.0130(9)
C8	4*e*	1	0.3057(8)	0.4082(8)	0.3044(2)	0.015(1)
C9	4*e*	1	−0.3185(7)	0.1054(7)	−0.0242(2)	0.0119(9)
C10	4*e*	1	0.5120(7)	0.2061(7)	0.1122(2)	0.0078(8)
C11	4*e*	1	−0.0862(7)	0.0076(7)	0.1179(2)	0.0088(8)
C12	4*e*	1	0.6923(7)	0.6078(7)	0.2935(2)	0.0127(9)
C13	4*e*	1	−0.4678(8)	0.5131(7)	0.0250(2)	0.0122(9)
B1	4*e*	1	0.5925(8)	0.5576(8)	0.2485(2)	0.009(1)
B2	4*e*	1	−0.1439(9)	0.0210(9)	0.0690(2)	0.012(1)
B3	4*e*	1	0.1013(9)	0.7529(9)	0.2512(2)	0.014(1)
B4	4*e*	1	−0.3456(8)	0.5836(8)	0.0663(2)	0.010(1)
B5	4*e*	1	0.2745(9)	−0.1666(9)	0.0664(2)	0.012(1)
B6	4*e*	1	0.094(1)	0.396(1)	0.0726(2)	0.018(1)
B7	4*e*	1	−0.2717(8)	0.0830(9)	0.0260(2)	0.011(1)

Table 6
Selected interatomic distances (Å) in $Nd_{25}B_{14}C_{26}$.

Atoms	Distance	Atoms	Distance	Atoms	Distance
Nd1–C11	2.330(5)	Nd3–C4	2.666(7)	Nd5–B3	3.446(6)
C8	2.600(7)	C12	2.674(6)	B1	3.480(7)
C4	2.640(7)	B1	2.682(6)	Nd7	3.7798(4)
C5	2.649(7)	B1	2.816(7)	Nd11	3.7906(5)
B3	2.673(7)	C6	3.392(6)	Nd9	3.8231(4)
C12	2.704(6)	B3	3.395(7)	Nd12	3.831(1)
B3	2.828(7)	Nd11	3.5071(4)	Nd11	3.9565(4)
C5	3.351(6)	Nd9	3.6559(4)		
Nd2	3.4012(4)	Nd7	3.6598(4)	Nd6–C10	2.597(6)
B1	3.431(7)	Nd12	3.662(1)	C3	2.611(6)
Nd2	3.6180(5)	Nd11	3.6654(5)	C11	2.641(6)
Nd4	3.6215(4)	Nd5	3.7130(5)	C1	2.653(6)
Nd11	3.6675(5)	Nd6	3.7432(4)	C8	2.657(6)
Nd7	3.6899(4)	Nd5	3.9040(4)	B5	2.742(7)
Nd12	3.701(1)	Nd13	3.938(3)	B2	2.799(7)
Nd6	3.7451(4)			C9	2.921(6)
Nd5	3.7679(5)	Nd4 – C10	2.607(6)	B4	3.044(7)
Nd3	3.7966(5)	C11	2.620(6)	B7	3.230(7)
Nd5	3.8738(4)	C1	2.654(6)	Nd11	3.6014(4)
Nd13	3.934(3)	C5	2.688(6)	Nd10	3.6267(4)
		C7	2.689(7)	Nd7	3.7164(5)
Nd2–C1	2.370(5)	B2	2.793(7)	Nd13	3.753(3)
C8	2.571(7)	B4	2.819(7)	Nd9	3.7805(5)
C4	2.628(7)	B6	3.051(8)	Nd12	3.7914(9)
C6	2.658(6)	B7	3.139(7)	Nd10	3.8825(4)
C5	2.694(7)	Nd8	3.5131(4)		
B1	2.704(7)	Nd11	3.5294(4)	Nd7–C10	2.612(6)
B3	2.876(7)	Nd9	3.6589(5)	C7	2.630(7)
C12	3.350(6)	Nd6	3.6853(5)	C3	2.656(6)
B3	3.429(7)	Nd7	3.7381(5)	C11	2.695(6)
Nd9	3.6304(4)	Nd12	3.7635(7)	B6	2.705(8)
Nd4	3.6443(4)	Nd13	3.792(3)	C12	2.777(6)
Nd3	3.6666(5)	Nd10	3.8092(4)	B5	2.827(7)
Nd12	3.668(1)	Nd5	3.8098(4)	C2	2.848(9)
Nd6	3.7037(4)			B2	3.000(7)
Nd5	3.7496(5)	Nd5–C7	2.452(6)	Nd11	3.4975(4)
Nd11	3.8504(5)	C4	2.613(7)	Nd14	3.5234(3)
Nd13	3.902(3)	C12	2.647(6)	Nd9	3.6350(5)
Nd5	3.9042(4)	C6	2.662(6)	Nd12	3.7442(7)
		C5	2.664(7)	Nd10	3.7609(4)
Nd3–C3	2.360(5)	C8	2.924(6)	Nd13	3.765(3)
C8	2.605(7)	B1	3.375(7)		
C6	2.646(6)	B3	3.400(7)		
Nd8–C2	2.663(9)	Nd10–B7	2.768(7)	Nd13–C4	3.182(7)
C2	2.724(9)	C13	2.800(6)	Nd14	3.829(3)
C9	2.729(6)	B7	2.846(7)		
B6	2.753(7)	C9	3.010(6)	Nd14–2B7	2.691(7)
C13	2.775(7)	B4	3.064(6)	2C9	2.699(6)
B5	2.795(7)	B2	3.529(7)	2B2	2.708(7)
C13	2.828(7)	Nd14	3.7428(3)	2C2	2.902(9)
B7	2.914(7)	Nd10	3.9928(5)	2B5	2.952(7)
B4	3.064(6)				
B6	3.067(7)	Nd11–C10	2.351(5)	C1–B4	1.448(8)
Nd9	3.5092(4)	C8	2.558(7)		
Nd8	3.5535(5)	C12	2.642(6)	C2–B6	1.50(1)
Nd10	3.7094(5)	C5	2.651(7)		
Nd14	3.7166(3)	C6	2.673(6)	C3–B5	1.475(8)
Nd10	3.8780(5)	B3	2.700(7)		
Nd13	3.880(3)	B1	2.935(7)	C4–B3	1.465(9)
Nd13	3.886(3)	C4	3.439(6)		
		B1	3.440(7)	C5–B3	1.460(9)
Nd9–C10	2.576(6)				
C7	2.654(7)	Nd12–C7	2.618(7)	C6–B1	1.450(8)
C1	2.669(6)	C3	2.643(6)		
C6	2.694(6)	C1	2.647(6)	C7–B6	1.458(8)
C3	2.709(6)	C11	2.666(6)		
B6	2.742(8)	C4	2.827(6)	C9–B7	1.488(8)
B4	2.816(7)	B6	2.970(8)		
C13	3.067(6)	B5	3.019(7)	C11–B2	1.443(8)
B5	3.165(7)	B2	3.021(7)		
C2	3.234(9)	B4	3.096(7)	C12–B1	1.459(8)
Nd11	3.5410(4)				
Nd12	3.7401(9)	Nd13–C1	2.665(7)	C13–C13	1.490(8)
Nd10	3.7446(4)	C11	2.689(6)	B4	1.506(8)
Nd13	3.807(3)	C3	2.721(7)		
		C7	2.724(7)	B2–B7	1.535(9)
Nd10–C2	2.638(9)	B2	2.868(8)		
C9	2.714(6)	B6	2.895(9)		
C13	2.735(6)	B5	2.914(8)		
C10	2.743(5)	B4	2.944(7)		

Table 7
Selected interatomic distances (Å) in $Nd_{25}B_{12}C_{28}$.

Atoms	Distance	Atoms	Distance	Atoms	Distance
Nd1–C1	2.60(1)	C15	2.68(1)	Nd28	3.4456(8)
C15	2.65(1)	C11	2.72(1)	Nd13	3.6388(8)
C13	2.66(1)	B3	2.77(1)	Nd6	3.6507(8)
C8	2.73(1)	B1	2.82(1)	Nd26	3.6951(8)
B6	2.75(1)	B6	3.02(1)	Nd10	3.775(3)
C9	2.75(1)	Nd20	3.5141(8)	Nd11	3.793(2)
B1	2.79(1)	Nd15	3.5160(8)	Nd7	3.8176(8)
C26	3.05(1)	Nd21	3.6338(8)	Nd22	3.8991(8)
B2	3.18(1)	Nd25	3.6397(8)		
C27	3.19(1)	Nd12	3.6872(8)	Nd6–C17	2.37(1)
Nd20	3.5205(8)	Nd4	3.7269(8)	C18	2.57(1)
Nd15	3.5530(8)	Nd17	3.756(1)	C6	2.65(1)
Nd4	3.6348(8)	Nd22	3.8063(8)	B10	2.66(1)
Nd25	3.6394(8)	Nd18	3.808(7)	C4	2.66(1)
Nd28	3.6451(8)	Nd8	3.8352(8)	C3	2.70(1)
Nd3	3.6651(8)			B9	2.78(1)
Nd17	3.747(1)	Nd4–C1	2.62(1)	Nd15	3.5000(8)
Nd8	3.7575(8)	C15	2.64(1)	Nd7	3.6314(8)
Nd12	3.7705(8)	C8	2.65(1)	Nd19	3.6565(8)
Nd22	3.8087(8)	C12	2.67(1)	Nd13	3.6586(8)
Nd18	3.821(7)	B6	2.71(1)	Nd16	3.6785(8)
		C10	2.79(1)	Nd11	3.766(2)
Nd2–C2	2.33(1)	C27	2.81(1)	Nd27	3.810(1)
C18	2.57(1)	B2	2.82(1)	Nd22	3.8807(8)
C3	2.65(1)	B3	2.99(1)		
C14	2.66(1)	Nd15	3.5139(8)	Nd7–C5	2.37(1)
B5	2.69(1)	Nd29	3.5297(6)	C18	2.56(1)
C6	2.71(1)	Nd21	3.6701(8)	C14	2.64(1)
B12	2.82(1)	Nd12	3.7253(8)	C3	2.64(1)
Nd25	3.4253(8)	Nd17	3.747(1)	C4	2.66(1)
Nd5	3.6096(8)	Nd18	3.752(2)	B9	2.70(1)
Nd16	3.6490(8)	Nd8	3.7555(8)	B5	2.91(1)
Nd7	3.6548(8)	Nd22	3.7752(8)	Nd21	3.4127(8)
Nd19	3.6598(8)			Nd19	3.6158(8)
Nd26	3.7016(8)	Nd5–C7	2.36(1)	Nd13	3.6561(8)
Nd10	3.752(2)	C18	2.58(1)	Nd26	3.6936(8)
Nd11	3.819(2)	C14	2.65(1)	Nd27	3.746(1)
Nd6	3.8279(8)	C6	2.65(1)	Nd11	3.795(2)
Nd22	3.8734(8)	C4	2.66(1)	Nd22	3.9282(8)
		B12	2.68(1)		
Nd3–C1	2.58(1)	B10	2.88(1)	Nd8–C27	2.62(1)
C12	2.62(1)	C20	3.30(1)	C22	2.74(1)
C13	2.67(1)	B9	3.42(1)	C26	2.74(1)
Nd8–C1	2.77(1)	Nd10–Nd25	3.997(5)	Nd13–Nd27	3.7963(9)
C24	2.77(1)			Nd24	3.984(9)
C26	2.78(1)	Nd11–C16	2.59(2)		
C24	2.87(1)	C4	2.62(1)	Nd14–2C25	2.69(1)
C22	2.99(1)	C3	2.64(1)	2C23	2.71(1)
B1	3.07(1)	C6	2.66(1)	2B4	2.71(1)
Nd12	3.6434(8)	C14	2.67(1)	2C28	2.87(2)
Nd20	3.7172(8)	C19	2.84(2)	2B7	2.95(1)
Nd29	3.7323(6)	Nd21	3.699(6)	2Nd19	3.5443(6)
Nd12	3.8552(8)	Nd28	3.726(6)	2Nd24	3.665(1)
Nd20	3.8640(8)	Nd25	3.740(6)	2Nd23	3.740(1)
Nd8	3.9900(8)	Nd15	3.771(6)	2Nd27	3.9689(8)
		Nd16	3.947(6)		
Nd9–C28	2.70(2)	Nd13	3.951(6)	Nd15–C1	2.35(1)
C23	2.70(1)	Nd19	3.961(6)	C16	2.56(1)
B11	2.71(2)			C10	2.60(1)
C21	2.75(1)	Nd12–C1	2.60(1)	C11	2.65(1)
C28	2.77(2)	C8	2.60(1)	C9	2.69(1)
B7	2.79(1)	C12	2.65(1)	B5	2.70(1)
C21	2.82(1)	C13	2.65(1)	B9	2.90(1)
C25	2.87(1)	B2	2.73(1)	Nd28	3.6673(8)
B11	3.02(2)	B3	2.77(1)	Nd21	3.6824(8)
B8	3.05(1)	C22	2.95(1)	Nd22	3.7849(8)
Nd13	3.5376(8)	B1	3.04(1)	Nd25	3.8362(8)
Nd16	3.5490(8)	Nd15	3.6251(8)		
Nd9	3.5732(8)	Nd28	3.7235(8)	Nd16–C19	2.55(2)
Nd24	3.672(1)	Nd25	3.7291(8)	C2	2.61(1)
Nd23	3.728(1)	Nd18	3.743(3)	C7	2.65(1)
Nd14	3.7327(6)	Nd21	3.7754(8)	C17	2.69(1)
Nd23	3.846(1)	Nd17	3.784(2)	C6	2.73(1)
Nd24	3.857(1)			B4	2.79(1)
		Nd13–C19	2.57(2)	B8	2.86(1)

Table 7 (*continued*)

Atoms	Distance	Atoms	Distance	Atoms	Distance
Nd10–C19	2.47(2)	C7	2.63(1)	C25	3.110(12)
C14	2.61(1)	C17	2.66(1)	Nd2	3.6564(8)
C6	2.64(1)	C4	2.68(1)	Nd19	3.7462(8)
C3	2.64(1)	C5	2.71(1)	Nd23	3.794(1)
C4	2.64(1)	B11	2.79(2)	Nd27	3.8038(9)
C16	2.96(2)	B8	2.81(1)		
Nd16	3.660(5)	C21	3.08(1)	Nd17–C15	2.62(1)
Nd19	3.694(5)	Nd16	3.6450(8)	C13	2.64(1)
Nd13	3.698(5)	Nd19	3.6519(8)	C8	2.64(1)
Nd26	3.772(5)	Nd26	3.7413(8)	C12	2.67(1)
Nd21	3.961(5)	Nd23	3.773(1)	C20	2.90(2)
Nd17–B6	2.96(1)	Nd20–C26	2.82(1)	Nd24–C28	2.63(2)
B2	3.01(1)	C24	2.92(1)	C21	2.72(1)
B3	3.02(1)	B1	3.06(1)	C23	2.75(1)
B1	3.08(1)	B6	3.06(1)	C25	2.76(1)
Nd25	3.656(4)	C26	2.78(1)	C21	2.77(1)
Nd28	3.671(4)	B2	2.82(1)	C25	2.84(2)
Nd21	3.716(4)	Nd20	3.5359(8)	B8	2.85(2)
Nd22	3.853(5)	Nd29	3.7280(6)	C23	2.92(2)
				Nd24	3.894(1)
Nd18–C13	2.67(1)	Nd21–C12	2.34(1)	Nd26	3.926(9)
C12	2.69(1)	C16	2.62(1)		
C8	2.72(1)	B12	2.64(1)	Nd25–C13	2.35(1)
C15	2.75(1)	C20	2.66(1)	C16	2.60(1)
B3	2.86(2)	C11	2.67(1)	C9	2.64(1)
B2	2.89(2)	C10	2.72(1)	C20	2.65(1)
B6	2.90(2)	B5	2.86(1)	C11	2.68(1)
B1	2.94(2)	Nd25	3.6255(8)	B10	2.70(1)
Nd29	3.792(1)	Nd22	3.7552(8)	B12	2.85(1)
Nd20	3.853(1)	Nd28	3.7846(8)		
Nd20	3.869(1)			Nd26–C5	2.59(1)
Nd25	3.915(1)	Nd22–C15	2.43(1)	C19	2.64(2)
Nd28	3.954(1)	C20	2.61(1)	C2	2.64(1)
Nd21	3.955(1)	C11	2.65(1)	C7	2.67(1)
		C10	2.65(1)	B7	2.76(1)
Nd19–C19	2.63(2)	C9	2.67(1)	C14	2.78(1)
C17	2.64(1)	C18	2.92(1)	B4	2.83(1)
C5	2.65(1)	Nd28	3.7147(8)	Nd27	3.7601(9)
C2	2.68(1)	Nd25	3.7403(8)		
C3	2.72(1)			Nd27–C7	2.64(1)
B11	2.73(2)	Nd23–C28	2.61(2)	C17	2.65(1)
B7	2.85(1)	C21	2.72(2)	C5	2.66(1)
C28	2.85(2)	C23	2.73(2)	C2	2.67(1)
B4	3.04(1)	C25	2.75(2)	C18	2.77(1)
Nd26	3.7106(8)	C21	2.83(1)	B4	2.96(1)
Nd27	3.7510(9)	C25	2.90(2)	B7	2.99(1)
Nd23	3.772(1)	C19	2.91(2)	B8	3.00(1)
Nd24	3.964(1)	C23	2.99(2)	B11	3.01(2)
		B8	3.08(2)		
Nd20–C27	2.67(1)	Nd24	3.925(1)	Nd28–C8	2.36(1)
C22	2.70(1)	Nd23	3.98(1)	C16	2.58(1)
B6	2.76(1)	Nd26	3.994(9)	C20	2.63(1)
C27	2.77(1)			C9	2.64(1)
Nd28–B10	2.86(1)	C8–B2	1.45(2)	C21–C21	1.48(2)
				B8	1.51(2)
Nd29–2C24	2.69(1)	C9–B10	1.47(2)		
2C22	2.69(1)			C22–C24	1.51(2)
2B3	2.72(1)	C10–B9	1.45(2)	B2	1.53(2)
2C27	2.93(1)				
2B2	2.97(1)	C11–B5	1.46(2)	C23–B7	1.50(2)
				C25	1.51(2)
C2–B4	1.48(2)	C12–B3	1.43(2)		
				C24–B3	1.52(2)
C3–B5	1.46(2)	C13–B1	1.46(2)		
				C25–B4	1.50(2)
C4–B9	1.49(2)	C14–B12	1.49(2)		
				C26–C26	1.49(2)
C5–B7	1.48(2)	C15–B6	1.47(2)	B1	1.52(2)
C6–B10	1.43(2)	C17–B11	1.44(2)	C27–B6	1.49(2)
C7–B8	1.49(2)	C20–B12	1.46(2)	C28–B11	1.44(2)

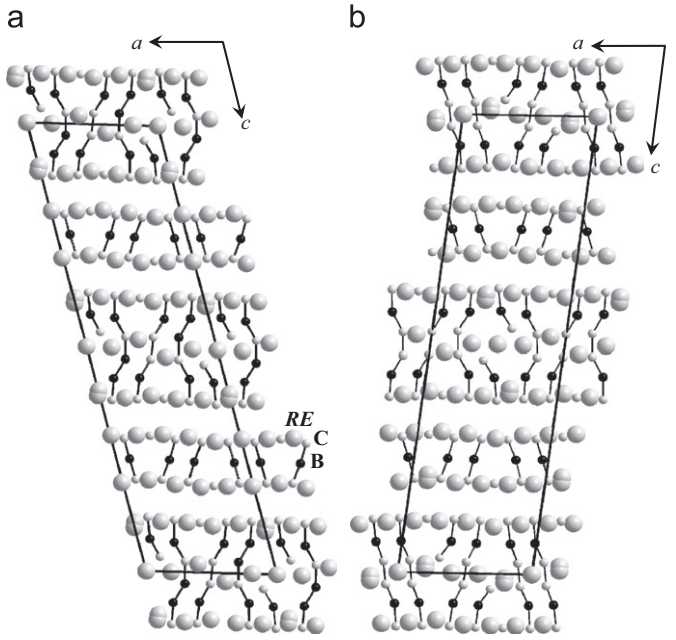

Fig. 2. Crystal structures of $RE_{25}B_{14}C_{26}$ (a) and $Nd_{25}B_{12}C_{28}$ (b) along [0 1 0], B, C units enhanced.

45°. Such a stacking leads to the formation of four different types of cavities: (i) octahedral, (ii) distorted bicapped square-antiprismatic, (iii) distorted monocapped square-antiprismatic, and (iv) distorted bicapped double antiprismatic cavities encapsulating isolated carbon atoms, BC_2 chains, B_2C_4 and B_3C_3 oligomers, respectively (see Fig. 3i–iv).

In the metal atom framework of $Nd_{25}B_{12}C_{26}$ the Nd–Nd distances between the nets range from 3.5131(4) Å (Nd8–Nd4) to 4.107(1) Å (Nd14–Nd12). Within the nets, the Nd–Nd separations are somewhat shorter, between 3.553(1) Å (Nd8–Nd8) and 3.878(1) Å (Nd8–Nd10) (see Table 6). Similar Nd–Nd distances were also found in the metal atom framework of $Nd_{25}B_{12}C_{28}$ (see Table 7).

The non-metal part of the structure of $RE_{25}B_{14}C_{26}$, (RE=Pr, Nd) (Fig. 2a) contains two types of slabs. One slab is formed from nearly linear and finite CBC units an cavities (ii) and isolated carbon atoms in cavities (i) whereas the other is formed from B_2C_4, B_3C_3, both in cavities (iv), bent CBC in cavities (iii) and isolated carbon atoms in holes (i).

The triclinic structure $Nd_{25}B_{12}C_{28}$ (Fig. 2b) also contains two types of slabs. One slab is similar to that in $RE_{25}B_{14}C_{26}$ and formed from nearly linear CBC units in cavities (ii) and isolated carbon atoms in holes (i) whereas the other slab is different to that in $RE_{25}B_{14}C_{26}$ and formed from B_2C_4 in cavities (iv), bent CBC entities in cavities (iii) and isolated carbon atoms in cavities (i).

The carbon atoms of the nearly linear CBC unit in $RE_{25}B_{14}C_{26}$ and $Nd_{25}B_{12}C_{28}$ exhibit long distances to apical RE atoms and almost identical short distances to equatorial RE atoms, on average 2.65 Å (Fig. 3ii, Tables 6 and 7). B–C distances (C_x–B_y=X Å and C_z–B_y=Y Å) are in the range of those generally measured in this kind of compound. The C–B–C angles are on average 175°.

The bent CBC units (Fig. 3iii) show C–B–C angles of 146.3(9)° for $Nd_{25}B_{12}C_{28}$ and 148.7(7)° for $Nd_{25}B_{14}C_{26}$. The distances are presented in Tables 6 and 7. Similar bent CBC units are observed in quarternary phases, such as $La_9Br_5B_3C_6$ [30], $La_4I_5B_2C$ [31], and $La_3Br_2BC_2$ [31] with C–B–C angles ranging from 141° to 151°. Besides the CBC units in $RE_{25}B_{14}C_{26}$, six-atom non-metal units are found in the same slab: Two symmetrical B_2C_4 units (C1–B4–C13–C13–B4–C1) and four asymmetrical B_3C_3 units (C11–B2–B7–C9–B5–C3, C3–B5–C9–B7–B2–C11). B–C distances in B_2C_4 units range from 1.447(8) Å (C1–B4) to 1.505(9) Å (C13–B4) with corresponding bond angles $\varphi_{C1-B4-C13}$=152.9(7)° to $\varphi_{C13-C13-B4}$=152.4(7)°.

In contrast the structure of $Nd_{25}B_{12}C_{28}$ contains only six B_2C_4 units beside CBC entities. Two are symmetrical (C13–B1–C26–C26–B1–C13, C7–B8–C21–C21–B8–C7) and four asymmetrical (C8–B2–C22–C24–B3–C12, C2–B4–C25–C23–B7–C5). B–C distances in the B_2C_4 entities range from 1.42(1) Å (C12–B3) to 1.53(1) Å (C12–B2) (see Table 7), and the averaged C–C distance is 1.49 Å. Bond angles in the units range from $\varphi_{C12-B3-C24}$=150.6(9)° to $\varphi_{C13-B1-C26}$=153.1(9)°.

Nearly similar bond lengths are measured for identical B_2C_4 entities in $Nd_{15}B_6C_{20}$ with B–C distances ranging from 1.41 to 1.54 Å and an averaged C–C distance of 1.48 Å [20]. In the B_3C_3 unit of $Nd_{25}B_{14}C_{26}$ the B2–B7 distance is 1.54(1) Å, and B–C distances range from 1.443(8) to 1.514(8) Å (see Table 6). This kind of B_3C_3 unit with nearly similar bond lengths is known only in the $RE_5B_4C_5$ structures [18]. The B–C distances in $RE_{25}B_{14}C_{26}$ (RE=Pr, Nd) and $Nd_{25}B_{12}C_{28}$ are comparable to those typically found for other related rare-earth metal boride carbides containing finite boride carbide anions [1] (see Tables 6 and 7).

Unambiguous location of B and C atoms in this kind of compounds is not obvious only from X-ray measurements, but often decided on the basis of the metal atom coordination, the electronegativity of B *vs.* C and also theoretical considerations [1,3–5]. With respect to this point, two structural aspects need to be addressed: The boron *vs.* carbon distribution in the B_2C_4 units (C–B–C–C–B–C, as experimentally proposed, or alternatively C–C–B–B–C–C) and substitution of carbon *vs.* boron in the six-atom non-metal units (C–B–B–C–B–C, as experimentally proposed, or C–B–B–B–C–C). Polyanions $[B_2C_4]^{6-}$ and $[B_3C_3]^{7-}$, nearly linear $[BC_2]^{5-}$and bent $[BC_2]^{7-}$ units isoelectronic with CO_2 and SO_2, respectively, could be formulated [5,20,30], leading to a charge distribution for $RE_{25}B_{14}C_{26}$ as: $(RE^{3+})_{25}[B_2C_4]^{6-}([B_3C_3]^{7-})_2([BC_2]^{5-})_4([BC_2]^{7-})_2(C^{4-})_4\cdot 5e^-$ and for $Nd_{25}B_{12}C_{28}$: $(Nd^{3+})_{25}([B_2C_4]^{6-})_3([BC_2]^{5-})_4([BC_2]^{7-})_2\,(C^{4-})_4\cdot 7e^-$.

3.2. Electronic structure

Previous theoretical studies on rare-earth metal boride carbides have shown that their structures can be rationalized within the approximation of a purely ionic bonding mode between the metal and the non-metal elements [1,3–5]. Using the same approach to study the chemical bonding in $RE_{25}B_{14}C_{26}$ and $Nd_{25}B_{12}C_{28}$ compounds leads us to the question of the assignment of formal ionic charges. If we assume the charge distribution mentioned above, five and seven electrons remain available for metal–metal bonding in $RE_{25}B_{14}C_{26}$ and $Nd_{25}B_{12}C_{28}$, respectively. DOS curves for both neodymium compounds are shown in Fig. 4. Both DOS curves present the same features as expected, since both compounds exhibit similar crystal structures. The participation of metallic atoms in levels below the Fermi level demonstrates the covalent interaction between the metal and the non-metal elements. As in many compounds containing finite boron–carbon units, the Fermi level cut a narrow DOS peak in both compounds that results from the overlapping between the bottom of the metallic d-band and the "intermediate" p-type orbitals of the boron–carbon anionic entities. Metallic properties are foreseen for both compounds.

Since another B/C distribution can be envisioned in B_2C_4 units of $RE_{25}B_{14}C_{26}$ and $Nd_{25}B_{12}C_{28}$ compounds, namely C–C–B–B–C–C, these structural hypotheses were also computed. Both compounds are energetically less stable by more than 2.5 eV/formula with such a distribution. Even if total energies computed with the EH semi-empirical method must be considered cautiously, these differences are significantly large to discard this alternative B/C

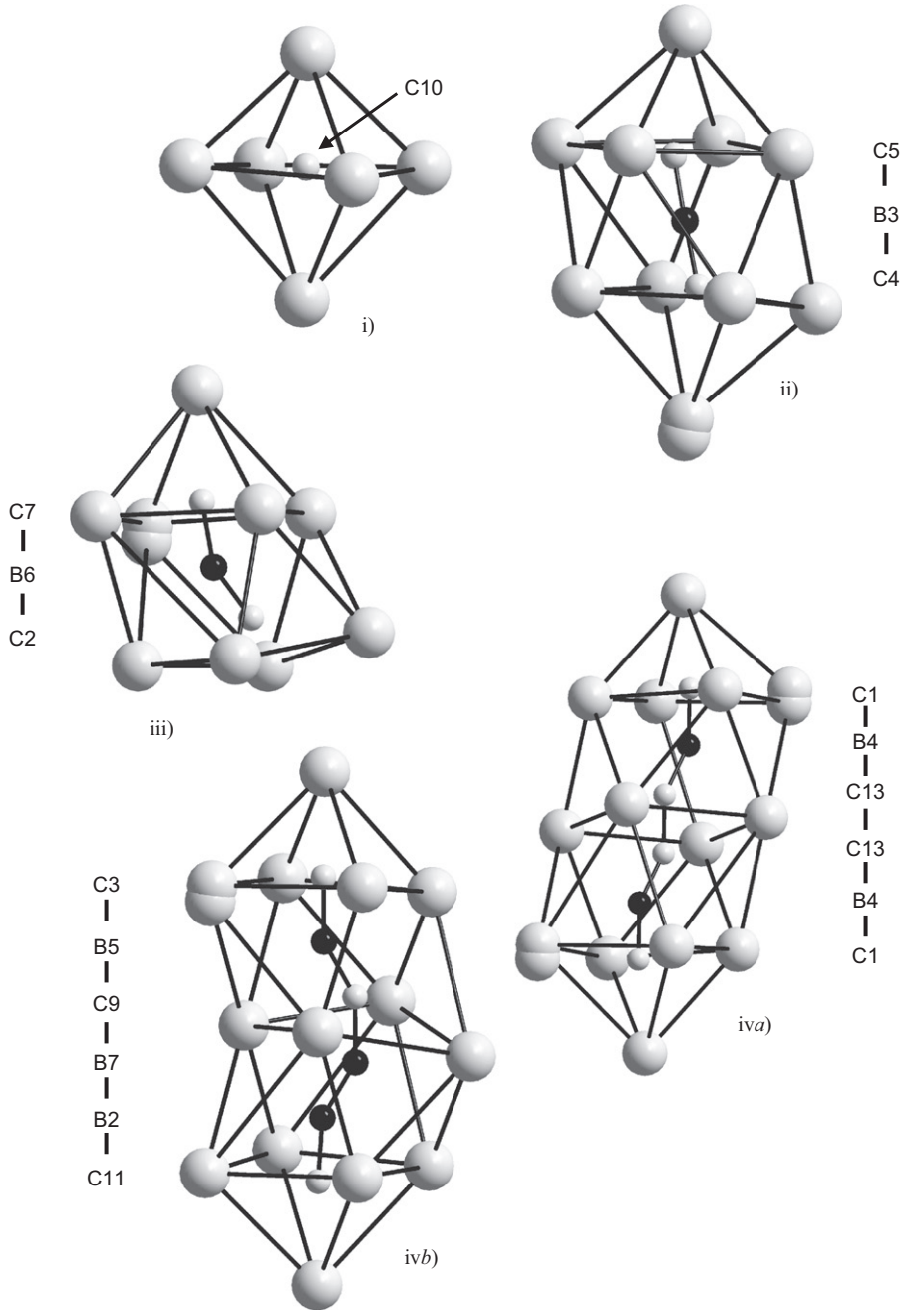

Fig. 3. Arrangement of the quasi-molecular boron–carbon entities in $RE_{25}B_{14}C_{26}$ and their rare-earth metal atom environments: isolated carbon atoms (i), nearly linear (ii) and bent (iii) BC_2 units, B_2C_4 (iv*a*) and B_3C_3 (iv*b*). Boron and carbon atom labeling correspond to that given in Table 6.

distribution. This discussion would certainly gain in importance with quantitative arguments based on results obtained from first-principles methods. Unfortunately, attempts to calculate the density functional theory band structure of both arrangements failed using the TB-LMTO-ASA program [32].

4. Conclusion

The compounds $RE_{25}B_{14}C_{26}$ (RE=Pr, Nd) and $Nd_{25}B_{12}C_{28}$ can be prepared at high temperatures by arc-melting and subsequent remelting in a high-frequency furnace from the elements. The temperature region of existence of $RE_{25}B_{14}C_{26}$ (RE=Pr, Nd) and $Nd_{25}B_{12}C_{28}$ is higher than 1270 K. At 1270 K they decompose into other ternary boride carbides stable at this temperature. The structures consist of a three-dimensional framework of rare-earth metal atoms resulting from the stacking of slightly corrugated and distorted square nets, leading to cavities filled with B_3C_3, B_2C_4, linear and bent CBC finite units as well as isolated carbon atoms. Structural and theoretical analysis suggests the ionic formulation for $RE_{25}B_{14}C_{26}$: $(RE^{3+})_{25}[B_2C_4]^{6-}([B_3C_3]^{7-})_2([BC_2]^{5-})_4([BC_2]^{7-})_2$ $(C^{4-})_4\cdot 5e^-$ and for $Nd_{25}B_{12}C_{28}$: $(Nd^{3+})_{25}([B_2C_4]^{6-})_3([BC_2]^{5-})_4([BC_2]^{7-})_2(C^{4-})_4\cdot 7e^-$ with rare-earth metals not fully oxidized. Accordingly, EH-TB calculations indicate that the title compounds are metallic in character. Semi-empirical calculations on different boron *vs.* carbon distributions show that the

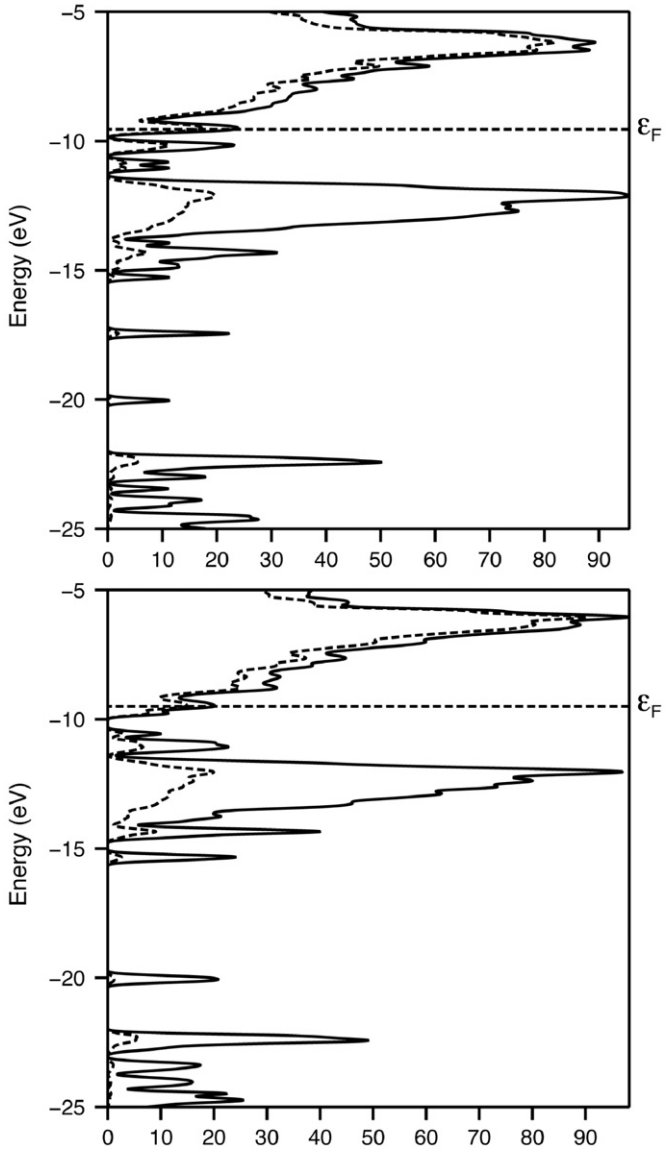

Fig. 4. Total density of states (solid line) and metal contribution (dashed line) for $Nd_{25}B_{14}C_{26}$ (top) and $Nd_{25}B_{12}C_{28}$ (bottom) obtained from EH-TB calculations.

crystal structures proposed on the basis of X-ray diffraction experiments are the most favorable.

Supplemental Information

Further details of the crystal structure investigation can be obtained from the Fachinformationszentrum Karlsruhe, 76344 Eggenstein-Leopoldshafen, Germany (fax: (49)7247-808-666; E-mail: crystdata@fiz-karlsruhe.de) on quoting the depository numbers CSD- 422787 for $Nd_{25}B_{12}C_{28}$, 422788 for $Nd_{25}B_{14}C_{26}$ and 422789 for $Pr_{25}B_{14}C_{26}$.

Acknowledgments

The authors gratefully thank M. Babizhetska for the sample preparation, H. Gärttling for X-ray intensity data collection.

References

[1] J. Bauer, J.-F. Halet, J.-Y. Saillard, Coord. Chem. Rev. 178–180 (1998) 723–753.
[2] T. Mori, Handbook on the Physics and Chemistry of Rare Earths, Higher borides, in: K.A. Gschneidner Jr., J.-C. Bunzli, V. Pecharsky (Eds.), North-Holland, Amsterdam, 2008, pp. 105–173.
[3] J.-F. Halet, Contemporary Boron Chemistry, in: M.G. Davidson, A.K. Hugues, T.B. Marder, K. Wade (Eds.), Royal Society of Chemistry, Cambridge, 2000, pp. 514–521 and Refs. therein.
[4] M. Ben Yahia, J. Roger, X. Rocquefelte, R. Gautier, J. Bauer, R. Guérin, J.-Y. Saillard, J.-F. Halet, J. Solid State Chem. 179 (2006) 2779–2786 and Refs. therein.
[5] (a) D. Ansel, J. Bauer, F. Bonhomme, G. Boucekkine, G. Frapper, P. Gougeon, J.-F. Halet, J.-Y. Saillard, B. Zouchoune, Angew. Chem. Int. Ed. 35 (1996) 2098–2101;
(b) J. Bauer, G. Boucekkine, G. Frapper, J.-F. Halet, J.-Y. Saillard, B. Zouchoune, J. Solid State Chem. 133 (1997) 190–194.
[6] F. Wiitkar, S. Kahlal, J.-F. Halet, J.-Y. Saillard, J. Bauer, P. Rogl, Inorg. Chem. 34 (1995) 1248–1256.
[7] F. Wiitkar, S. Kahlal, J.-F. Halet, J.-Y. Saillard, J. Bauer, P. Rogl, J. Am. Chem. Soc. 116 (1994) 251–261.
[8] (a) E. Zintl, Angew. Chem. 1 (1939) 52;
(b) W. Klemm, Proc. Chem. Soc. Lond. (1958) 329;
(c) H. Schäfer, B. Eisenmann, W. Müller, Angew. Chem. Int. Ed. 12 (1973) 694–712;
(d) S.M. Kauzlarich (Ed.), VCH, New York, 1996.
[9] (a) J.-F. Halet, J.-Y. Saillard, J. Bauer, J. Less-Comm. Metal. 158 (1990) 239–250;
(b) Y. Shi, A. Leithe-Jasper, T. Tanaka, J. Solid State Chem. 148 (1999) 250–259.
[10] (a) E. Bidaud, K. Hiebl, R. Hoffman, R. Pöttgen, C. Jardin, J. Bauer, R. Gautier, P. Gougeon, J.-Y. Saillard, J.-F. Halet, J. Solid State Chem. 154 (2000) 286–295;
(b) O. Oeckler, Hj. Mattausch, J. Bauer, A. Simon, Z. Naturforsch. 59b (2004) 1551–1562.
[11] V. Babizhetskyy, A. Simon, Hj. Mattausch, K. Hiebl, C. Zheng, J. Solid State Chem. 183 (2010) 2343–2351.
[12] O. Oeckler, C. Jardin, Hj. Mattausch, A. Simon, J.-F. Halet, J.-Y. Saillard, J. Bauer, Z. Anorg. Allg. Chem. 627 (2001) 1389–1394.
[13] Y. Shi, L. Bourgeois, A. Leithe-Jasper, Y. Bando, T. Tanaka, J. Alloys Compd. 298 (2000) 99–106.
[14] V. Babizhetskyy, J. Köler, Hj Mattausch, A. Simon, Z. Kristallogr. 226 (2011) 93–98.
[15] O. Oeckler, J. Bauer, Hj. Mattausch, A. Simon, Z. Anorg. Allg. Chem. 627 (2001) 779–788.
[16] P. Gougeon, J.-F. Halet, D. Ansel, J. Bauer, Z. Kristallogr. 211 (1996) 823.
[17] (a) P. Gougeon, J.-F. Halet, D. Ansel, J. Bauer, Z. Kristallogr. 211 (1996) 825;
(b) V. Babizhetskyy, K. Hiebl, R.K. Kremer, Hj. Mattausch, A. Simon, Solid State Sci. 9 (2007) 1126–1134.
[18] (a) P. Gougeon, J.-F. Halet, D. Ansel, J. Bauer, Z. Kristallogr. 211 (1996) 822;
(b) V. Babizhetskyy, Hj. Mattausch, A. Simon, Z. Kristallogr. 218 (2003) 417–418;
(c) V. Babizhetskyy, K. Hiebl, Hj. Mattausch, A. Simon, J. Phys. Chem. Solids 70 (2009) 561–566.
[19] (a) V. Babizhetskyy, Hj. Mattausch, R. Gautier, J. Bauer, J.-F. Halet, A. Simon, Z. Anorg. Allg. Chem. 631 (2005) 1041–1046;
(b) V. Babizhetskyy, K. Hiebl, Hj. Mattausch, A. Simon, Solid State Sci. 11 (2009) 501–506.
[20] V. Babizhetskyy, Hj. Mattausch, A. Simon, K. Hiebl, M. Ben Yahia, R. Gautier, J.-F. Halet, J. Solid State Chem. 181 (2008) 1882–1890.
[21] V. Babizhetskyy, H.J. Mattausch, A. Simon, in: Proceedings of the IXth International Conference of Intermetallic Compounds, Lviv, Ukraine, 20–24 September 2005, p. 31.
[22] V. Babizhetskyy, Hj. Mattausch, A. Simon, Z. Kristallogr. 221 (2006) 1.
[23] L.G. Akselrud, Yu.N. Grin, P.Yu. Zavalii, V.K. Pecharskii, WinCSD—Universal Program Package for single crystal and/or powder structure data treatment, Materials Science Forum 335 (1993) 133.
[24] A. Altomare, M.C. Burla, M. Camalli, G.L. Cascarano, C. Giacovazzo, A. Guagliardi, A.G. Giuseppina Moliterni, G. Polidori, R. Spagna, J. Appl. Crystallogr. 32 (1999) 115–119.
[25] G.M. Sheldrick, SHELXL-97, Program for the Refinement of Crystal Structures, University of Göttingen, Germany, 1997.
[26] L.J. Farrugia, WinGX (Version 1.64.05), J. Appl. Crystallogr 32 (1999) 837–838.
[27] K. Brandenburg, DIAMOND (Version 2.1d), Crystal Impact GbR, Bonn, Germany 1996–2001.
[28] (a) R. Hoffmann, J. Chem. Phys. 39 (1963) 1397–1412;
(b) M.-H. Whangbo, R. Hoffmann, J. Am. Chem. Soc. 100 (1978) 6093–6098.
[29] G.A. Landrum, YAeHMOP, Yet Another extended Hückel Molecular Orbital Package, release 2.0, Cornell University, Ithaca, NY, 1997.
[30] Hj. Mattausch, A. Simon, C. Felser, R. Dronskowski, Angew. Chem. 108 (1996) 1805–1807.
[31] Hj. Mattausch, O. Oeckler, A. Simon, Inorg. Chim. Acta 289 (1999) 174–190.
[32] R.W. Tank, O. Jepsen, A. Burkhardt, O.K. Andersen, The STUTTGART TB-LMTO-ASA program, Version 4.7; Max-Planck-Institut für Festkörperforschung: Stuttgart, Germany, 1999.